Steel and Composite Structures, *Vol. 32, No. 3 (2019) 293-304*
DOI: https://doi.org/10.12989/scs.2019.32.3.293

Nonlocal geometrically nonlinear dynamic analysis of nanobeam using a meshless method

Mohammad Hossein Ghadiri Rad [*1], Farzad Shahabian [2a] and Seyed Mahmoud Hosseini [3b]

[1] *Civil Engineering Department, Quchan University of Technology, Quchan, Iran*
[2] *Civil Engineering Department, Faculty of Engineering, Ferdowsi University of Mashhad, Mashhad, Iran*
[3] *Industrial Engineering Department, Faculty of Engineering, Ferdowsi University of Mashhad, Mashhad, Iran*

(*Received October 18, 2018, Revised May 28, 2019, Accepted July 10, 2019*)

Abstract. In the present paper, the element free Galerkin (EFG) method is developed for geometrically nonlinear analysis of deep beams considering small scale effect. To interpret the behavior of structure at the nano scale, the higher-order gradient elasticity nonlocal theory is taken into account. The radial point interpolation method with high order of continuity is used to construct the shape functions. The nonlinear equation of motion is derived using the principle of the minimization of total potential energy based on total Lagrangian approach. The Newmark method with the small time steps is used to solve the time dependent equations. At each time step, the iterative Newton-Raphson technique is applied to minimize the residential forces caused by the nonlinearity of the equations. The effects of nonlocal parameter and aspect ratio on stiffness and dynamic parameters are discussed by numerical examples. This paper furnishes a ground to develop the EFG method for large deformation analysis of structures considering small scale effects.

Keywords: cnonlocal elasticity; element-free Galerkin (EFG) method; dynamic analysis; total Lagrangian approach; geometrically nonlinear analysis

1. Introduction

In recent decades the application of nanotechnology in many industrial applications in two ways including the use of nano-materials for reinforcement and nanostructures has been increased. Numerous works on reinforcing structures by nano-materials have been reported in literatures in the various fields such as dynamic analysis (Lei *et al*. 2015, Zhang and Selim 2017 and Zhang *et al*. 2017), geometrically nonlinear analysis (Zhang and Liew 2015 and Zhang *et al*. 2016a), thermomechanical analysis (Zhang *et al*. 2016b), buckling and stability analysis (Lei *et al*. 2014, Zhang *et al*. 2016c and Zhang 2017), postbuckling analysis (Zhang and Liew 2016 and Zhang *et al*. 2016d), composite plates (Zhang *et al*. 2015a and Zhang and Xiao 2017) and Piezoelectric (Zhang *et al*. 2016e). In these researches various numerical methods such as element free IMLS-Ritz method (Zhang *et al*. 2015b), local Petrov-Galerkin method (Zhu *et al*. 2014) and local Kriging meshless method (Zhang *et al*. 2014) have been used. The nanostructures because of their superior properties are implemented in high-tech devices. Experimental investigations on nanostructures show that the mechanical behavior of these structures can't be predicted by the ideal continuum theories due to neglecting the size effects (Ma and Clarke 1995, Poole *et al*. 1996, Chong *et al*. 2001, Chen *et al*. 2003, Cadek *et al*. 2004).

Several unconventional theories such as nonlocal couple stress (Mindlin 1964, Toupin 1964), modified couple stress (Yang *et al*. 2002, Akgöz and Civalek 2011), Eringen (1972a ,b) and strain gradient (Altan and Aifantis 1997, Aifantis 1999, Amanatidou and Aravas 2002, Lam *et al*. 2003) theories have been proposed to describe the mechanical behaviour of structures at the nanoscales. A brief review on nonlocal elasticity theories and related variational principles is presented by Polizzotto (2001).

There are a large number of papers in which the size effect are modelled using the nonlocal theories for various structures. For example, Darabi and Vosoughi (2016) presented an inverse hybrid numerical method for small scale parameter estimation of functionally graded nanobeams. Wang *et al*. (2017a) studied on small scale effect on both natural frequencies and vibration mode shapes of strain gradient nanobeams. They concluded that the natural frequency difference between that predicted by the strain gradient elastic beam and the classical beam rises with the increasing of the mode order and decreasing of the beam length. Bending and buckling of FG nanobeams with different higher order shear deformation theories is comprehensively studied by Rahmani *et al*. (2017). Wang *et al*. (2010) studied on the propagation characteristics of the longitudinal wave in nanoplates. They demonstrated that the longitudinal wave in nanoplates becomes dispersive and dispersion degree can be strengthened by increasing the scale coefficient.

The transverse nonlinear steady-state vibrations of the

∗Corresponding author, Assistant Professor,
E-mail: hosein_ghadiri@qiet.ac.ir
[a] Professor, E-mail: shahabf@um.ac.ir
[b] Professor, E-mail: sm_hosseini@um.ac.ir

ISSN: 1229-9367 (Print), 1598-6233 (Online)

double layered nanoplate (DLNP) with 3:1 internal resonance between the first two modes were investigated by Wang *et al*. (2017b). In their study, the method of multiple scales is employed to obtain the analytical nonlinear frequency-response relations. Wave propagation in functionally graded graphene platelets (FGGPLs)-reinforced nanocomposite thick hollow cylinder under shock loading is investigated by Hosseini and Zhang (2018b). Despotovic (2018) using Eringen's theory investigated the influence of body force and nonlocality on stability and free vibration of the nanoplates.

The vibration of non-uniform nanoplates rested on elastic foundation is studied by Chakraverty and Behera (2015). Ghavanloo and Fazelzadeh (2016) presented an analytical method to evaluate Eringen's nonlocal parameter for single-walled carbon nanotubes. Some of the researchers have focused on size-dependent thermoelasticity of structures by combining the nonlocal and classical thermoelastic theories. Yu *et al*. (2016) investigated the effect of nonlocal parameter of elasticity and heat conduction on the critical load of nanobeams under non-uniform temperature. They concluded that the critical load is decreased by elastic nonlocal parameter and further decreased when thermal effect is taken into account. The thermal vibration behavior of two dimensional functionally graded nanobeams is studied by Mirjavadi *et al*. (2017). Hosseini (2018) for the first time developed an analytical solution for the coupled thermoelasticity analysis of a micro/nano beam resonator under shock loading based on the Green-Naghdi theory. The GN-based coupled thermoelasticity analysis of FG multilayer graphene platelets-reinforced nanocomposite cylinders is carried out by Hosseini and Zhang (2018a). The thermoelastic damping of nonlocal Euler–Bernoulli beam is carried out by Yu *et al*. (2017). They obtained the inverse quality factor by using the complex-frequency approach. A brief review on studies about the application of modified continuum elasticity theory in modeling of nanotubes, nanobeams, and nanoplates can be founded in Wang *et al*. (2016) article.

During the last decades several mesh-based methods have been presented for modelling small scale effect (Belytschko *et al*. 2009, Phadikar and Pradhan 2010, Taghizadeh *et al*. 2015, Nguyen *et al*. 2017, Nikkar *et al*. 2017, Arefi 2018). Despite the success of these methods, since in nonlocal theory the stresses at a point is a function of the strains at its all neighbour points (Eltaher *et al*. 2016), the meshless methods has the competitive advantage for nonlocal problems. Because comparing to the mesh-based methods, the discretization of domain for meshless methods is carried out using a set of scattered points. Recently published works shows that the meshless methods have attracted much attention to solve nonlocal problems. Askes and Aifantis (2002) implemented the Element-Free Galerkin method on theory of gradient elasticity to model size effects. They analyzed two boundary value problems including clamped beam under bending loading and square plate with hole under axial tension to show the capability of the gradient elasticity theory in capturing the size effects. Schwartz *et al*. (2012) proposed a boundary element coupled with local radial point interpolation method for analysis of 3D nonlocal elastic problems. Kiani (2014) using a nonlocal meshless method studied on the flexural vibrations of double-walled carbon nanotubes subjected to an initially axial force and embedded in an elastic matrix. An element free buckling analysis graphene sheets embedded in an elastic medium incorporating the non-local elasticity theory has been presented by Zhang *et al*. (2016c). They investigated the influence of nonlocal parameters, aspect ratio, side length and elastic foundation on the critical buckling load.

In some engineering problems, the nanostructures undergo large deformations so that the deformed shape of structure affects the results of problem. In such cases, the geometrically nonlinear analysis is unavoidable. Recently some studies have been conducted to analyse the large deformation of nanostructures using the nonlocal theory of elasticity. A nonlocal nonlinear finite element formulation of classical and shear deformation theories of beams and plates is presented by Reddy (2010). Malekzadeh and Shojaee (2013) studied on the surface and nonlocal effects on nonlinear free vibration of nano-beams. Wang *et al*. (2015a) by means of nonlocal theory and Von Kármán large deformation theory studied on homoclinic behaviors and chaotic motions of double layered viscoelastic nanoplates. In another work, they investigated the nonlinear flexural vibration properties of double layered viscoelastic nanoplates based on nonlocal continuum theory (Wang *et al*. 2015b). Gholami and Ansari (2016) based on Mindlin's plate theory and von Kármán geometric nonlinearity developed a nonclassical microplate method to investigate the size-dependent geometrically nonlinear free vibration of functionally graded microplates. Panyatong *et al*. (2018) developed a meshfree method for geometrically nonlinear analysis of the nanoplates. In their work, the effects of nonlocal parameter, von Kármán nonlinearity and aspect ratio on nonlinear bending are studied. Sladek *et al*. (2017) claimed to have given a formulation for large amplitude vibration of piezoelectroelastic nanoplates for the first time. They proposed a finite element formulation based on the Mindlin assumption and von Karman-type nonlinear field equations to analyse the piezoelectric nanoplate under a static and time-harmonic mechanical load and electric load. Wang *et al*. (2019), established the double mode nonlinear dynamical equations of the double layered nano plates subjected to transverse harmonic excitation and static in-plane compression by the nonlocal theory and von Kármán large deformation theory. From their formulation, it was rather novel that the rotary inertia could break the simplistic symmetry of the vibration system.

Compared to numerous works on the analysis of nanostructures considering small scale effect, a few work has been done on large deformation analysis of 2D (plane strain) structures. In this paper for the first time, the EFG method is developed for geometrically nonlinear analysis of nanostructures based on the higher-order gradient elasticity nonlocal theory. It should be mentioned that the EFG method is one of the most popular meshless methods because of its similarities with FEM. This technique is based on global weak form of governing differential equation. Though there exist a background cell for integration, there is no need to refine the integration cell when decreasing nodal distance for more accurate field approximation. Thus, the EFG method has high convergence rate and the computational time required for this method is less than other meshless methods. The gradient nonlocal elasticity theory is employed to model the size effect. In this method the stress of a node is a partial differential function of the strains at the all its neighbour points. In order to approximate this function, the radial basis function is used. It should be mentioned that, radial basis functions is suitable for estimating derivatives up to the second order. Geometrically nonlinear formulations are obtained with respect to the initial state of structure based on total lagrangian approach. The Newmark method is employed to discretize time domain and at each time step the iterative Newton-Raphson method is used to solve the nonlinear equations. Some numerical examples are analysed using proposed method and effect of nonlocal parameter on nonlinear dynamic behaviour of structure are studied in details. The results show that the EFG method is very effective method for large deformation analysis of nanostructures.

2. Gradient nonlocal elasticity theory

As previously mentioned, in gradient nonlocal elasticity theory proposed by Aifantis (1999) the stress field at a node in an elastic continuum is a function of strains at all its neighbor points which is expressed using the following partial differential equation.

$$S_{ij} = D_{ijkl}\left(1 - l^2\,\nabla^2\right)\left(\varepsilon_{kl}\right) \tag{1}$$

where, 'S_{ij}' is the second Piola–Kirchhoff stress tensor, '$l = e_0 a$' is the scale coefficient, '$\nabla^2 = \partial^2/\partial x^2 + \partial^2/\partial y^2$' is the Laplacian operator, 'D_{ijkl}' is the constitutive tensor and 'ε_{kl}' is the Cauchy strain tensor.

3. Geometrically nonlinear analysis

In geometrically nonlinear problems, the analysis is performed using an incremental-iterative procedure. At each incremental load step, the status of the body can be considered in two different state including initial and current configurations (see Fig. 1). The coordinates of a particle at the initial and current configurations are defined by 'X_i' and 'x_i', respectively. These coordinates are connected by the following relation.

$$x_i = X_i + u_i \tag{2}$$

where 'u_i' is 'i' directional displacement. In this paper, the geometrically nonlinear analysis is carried out using total Lagrangian approach where in the strains and stresses are measured with respect to the initial configuration. The deformation gradient tensor with respect to the initial configuration is given by

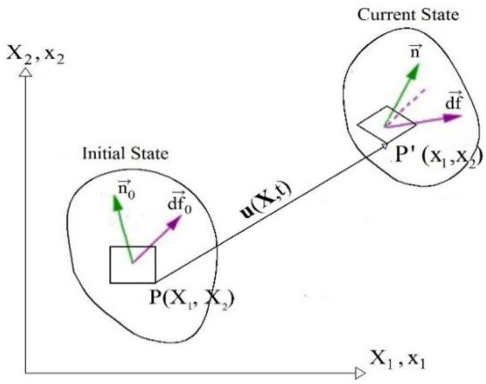

Fig. 1 Initial and current configurations in large deformation problems

$$F_{ij} = \frac{\partial x_i}{\partial X_j} = \delta_{ij} + \frac{\partial u_i}{\partial X_j} \tag{3}$$

Thus, the increment of deformation gradient tensor can be defined as

$$\Delta F_{ij} = \Delta\left(\frac{\partial u_i}{\partial X_j}\right) \tag{4}$$

The Cauchy strain tensor can be expressed in terms of deformation gradient tensor as follows.

$$\varepsilon_{ij} = \frac{1}{2}\left(F_{Ii}\,F_{Ij} - \delta_{ij}\right) \tag{5}$$

The derivative of the strain tensor (Eq. (5)), yields the following incremental equation.

$$\Delta\varepsilon_{ij} = \frac{1}{2}\left(\Delta F_{Ii}\,F_{Ij} - F_{Ii}\,\Delta F_{Ij}\right) \tag{6}$$

The expansion of Eq. (6) can be presented in the following matrix form. $\{\Delta\varepsilon\} = \left[\hat{F}\right]\{\Delta F\}$

$$\{\Delta\varepsilon\} = \left[\hat{F}\right]\{\Delta F\} \tag{7}$$

where

$$\left[\hat{F}\right] = \begin{bmatrix} F_{xx} & 0 & 0 & F_{yx} \\ 0 & F_{yy} & F_{xy} & 0 \\ F_{xy} & F_{yx} & F_{xx} & F_{yy} \end{bmatrix} \tag{8}$$

and

$$\{\Delta F\}^{\mathrm{T}} = \left\{\Delta F_{xx}\ \ \Delta F_{yy}\ \ \Delta F_{xy}\ \ \Delta F_{yx}\right\} \tag{9}$$

4. Discretizing the problem domain

In the meshless method, the shape functions are used to estimate the displacement function 'u' in terms of nodal displacement 'u_i'.

$$u = \sum_{i=1}^{n} \varphi_i u_i = [\varphi]^{\mathrm{T}} \{U\} \tag{10}$$

where, 'n' is the number of nodes in the support domain and 'φ_i' is the shape function. The radial point interpolation method (RPIM) is one of the most widely used method for construction the shape functions. In this method the shape function is defined as (Liu and Gu 2005)

$$[\varphi]^{\mathrm{T}} = [R]^{\mathrm{T}} \left[R_Q\right]^{-1} \tag{11}$$

where

$$\begin{cases} [R]^{\mathrm{T}} = [R_1 \;\; R_2 \;\; \cdots \;\; R_n] \\ \left[R_Q\right] = \begin{bmatrix} R_1(r_1) & R_2(r_1) & \cdots & R_n(r_1) \\ R_1(r_2) & R_2(r_2) & \cdots & R_n(r_2) \\ \vdots & \vdots & \ddots & \vdots \\ R_1(r_n) & R_2(r_n) & \cdots & R_n(r_n) \end{bmatrix} \end{cases} \tag{12}$$

In the last equation 'R_i' represents the radial basis function. In this paper, the multi-quadric (MQ) radial basis function with the following formulation is used to discretize the problem domain. This function has the Kronecker delta function property, and thus the application of essential boundary conditions is carried out in a simple way. Furthermore, the MQ function accurately estimates dependent variable up to the second order derivatives.

$$R_i = \left(r_i^2 + c^2\right)^q \tag{13}$$

in which 'r_i' denotes the distance between the point of interest and the nodes located in its support domain.

$$r_i = \left[(x - x_i)^2 + (y - y_i)^2\right]^{1/2} \tag{14}$$

Substituting Eq. (10) into Eq. (4), the linear strain matrix '$[B^l]$' (which gives the deformation gradient increment in terms of the nodal displacements increment) will be obtained.

$$\{\Delta F\} = \left[B^l\right]\{\Delta U\} \tag{15}$$

where

$$\left[B^l\right] = \begin{bmatrix} \varphi_{,x} & 0 \\ 0 & \varphi_{,y} \\ \varphi_{,y} & 0 \\ 0 & \varphi_{,x} \end{bmatrix} \tag{16}$$

Replacing Eq. (15) into Eq. (7), yields the nonlinear strain matrix '$[B^{nl}]$' (which gives the Cauchy strains in erms of nodal displacements increment).

$$\{\Delta \varepsilon\} = \left[B^{nl}\right]\{\Delta U\} \tag{17}$$

where

$$\left[B^{nl}\right] = \begin{bmatrix} F_{xx}\,\varphi_{,x} & F_{yx}\,\varphi_{,x} \\ F_{xy}\,\varphi_{,y} & F_{yy}\,\varphi_{,y} \\ F_{xy}\,\varphi_{,x} + F_{xx}\,\varphi_{,y} & F_{yx}\,\varphi_{,y} + F_{yy}\,\varphi_{,x} \end{bmatrix} \tag{18}$$

and

$$\{\Delta \varepsilon\}^{\mathrm{T}} = \left\{\Delta \varepsilon_{xx} \;\; \Delta \varepsilon_{yy} \;\; \Delta \gamma_{xy}\right\} \tag{19}$$

Finally, the gradient of the nonlinear strain matrix, which is used in nonlocal formulation, can be derived as the following equation.

$$\begin{aligned} \left[\nabla B^{nl}\right] &= \left(\frac{\partial}{\partial x} + \frac{\partial}{\partial y}\right)\left[B^{nl}\right] \\ &= \begin{bmatrix} F_{xx,x}\,\varphi_{,x} & F_{yx,x}\,\varphi_{,x} \\ F_{xy,x}\,\varphi_{,y} & F_{yy,x}\,\varphi_{,y} \\ F_{xy,x}\,\varphi_{,x} + F_{xx,x}\,\varphi_{,y} & F_{yx,x}\,\varphi_{,y} + F_{yy,x}\,\varphi_{,x} \end{bmatrix} \\ &+ \begin{bmatrix} F_{xx}\,\varphi_{,xx} & F_{yx}\,\varphi_{,xx} \\ F_{xy}\,\varphi_{,yx} & F_{yy}\,\varphi_{,yx} \\ F_{xy}\,\varphi_{,xx} + F_{xx}\,\varphi_{,yx} & F_{yx}\,\varphi_{,yx} + F_{yy}\,\varphi_{,xx} \end{bmatrix} \\ &+ \begin{bmatrix} F_{xx,y}\,\varphi_{,x} & F_{yx,y}\,\varphi_{,x} \\ F_{xy,y}\,\varphi_{,y} & F_{yy,y}\,\varphi_{,y} \\ F_{xy,y}\,\varphi_{,x} + F_{xx,y}\,\varphi_{,y} & F_{yx,y}\,\varphi_{,y} + F_{yy,y}\,\varphi_{,x} \end{bmatrix} \\ &+ \begin{bmatrix} F_{xx}\,\varphi_{,xy} & F_{yx}\,\varphi_{,xy} \\ F_{xy}\,\varphi_{,yy} & F_{yy}\,\varphi_{,yy} \\ F_{xy}\,\varphi_{,xy} + F_{xx}\,\varphi_{,yy} & F_{yx}\,\varphi_{,yy} + F_{yy}\,\varphi_{,xy} \end{bmatrix} \end{aligned} \tag{20}$$

5. Element free Galerkin method

In this section, the governing equation for the nonlocal geometrically nonlinear dynamic analysis is derived using the principle of the minimization of total potential energy. The statement of total potential energy function 'Π' at the initial configuration is given by

$$\begin{aligned} \Pi = \frac{1}{2}\int_{\Omega} \{\Delta \varepsilon\}^{\mathrm{T}} \{\Delta S\}\, \mathrm{d}\Omega + \int_{\Omega} \{\Delta \varepsilon\}^{\mathrm{T}} \{S_0\}\, \mathrm{d}\Omega \\ + \int_{\Omega} \{\Delta u\}^{\mathrm{T}} \rho \{\Delta \ddot{u}\}\, \mathrm{d}\Omega - \int_{\Gamma} \{\Delta u\}^{\mathrm{T}} \{\bar{t}\}\, \mathrm{d}\Gamma \end{aligned} \tag{21}$$

where '$\{\bar{t}\}$' is the traction vector, 'ρ' is the mass density and '$\{S_0\}$' is the initial second Piola–Kirchhoff stress vector. Substituting '$\{\Delta S\}$' from Eq. (1) into the last equation gives

$$\Pi = \frac{1}{2}\left(\int_{\Omega} \{\Delta \varepsilon\}^{\mathrm{T}} [D]\, \{\Delta \varepsilon\}\, \mathrm{d}\Omega\right. \tag{22}$$

$$
\left. - \int_{\Omega} \{\Delta\varepsilon\}^{\mathrm{T}} l^2 [D] \nabla^2 \{\Delta\varepsilon\} \, \mathrm{d}\Omega \right) + \int_{\Omega} \{\Delta\varepsilon\}^{\mathrm{T}} \{S_0\} \, \mathrm{d}\Omega + \int_{\Omega} \{\Delta u\}^{\mathrm{T}} \rho \{\Delta\ddot{u}\} \, \mathrm{d}\Omega - \int_{\Gamma} \{\Delta u\}^{\mathrm{T}} \{\bar{t}\} \, \mathrm{d}\Gamma \tag{22}
$$

where '$[D]$' is the constitutive matrix. The total potential energy function with lower order of derivatives can be obtained by applying divergence theorem to the recent equation.

$$
\begin{aligned}
\Pi = & \frac{1}{2} \int_{\Omega} \{\Delta\varepsilon\}^{\mathrm{T}} [D] \{\Delta\varepsilon\} \, \mathrm{d}\Omega \\
& - \frac{1}{2} \int_{\Gamma} \{\Delta\varepsilon\}^{\mathrm{T}} l^2 [D] \nabla \{\Delta\varepsilon\} \, \mathrm{d}\Omega \\
& + \frac{1}{2} \int_{\Omega} \nabla \{\Delta\varepsilon\}^{\mathrm{T}} l^2 [D] \nabla \{\Delta\varepsilon\} \, \mathrm{d}\Omega + \int_{\Omega} \{\Delta\varepsilon\}^{\mathrm{T}} \{S_0\} \, \mathrm{d}\Omega \\
& + \int_{\Omega} \{\Delta u\}^{\mathrm{T}} \rho \{\Delta\ddot{u}\} \, \mathrm{d}\Omega - \int_{\Gamma} \{\Delta u\}^{\mathrm{T}} \{\bar{t}\} \, \mathrm{d}\Gamma
\end{aligned} \tag{23}
$$

Assuming that the derivatives of strains vanish on the boundary (Askes and Aifantis 2002), the discretized form of Eq. (23) can be obtained using strain-displacement relation (Eq. (17)).

$$
\begin{aligned}
\Pi = & \frac{1}{2} \{\Delta U\}^{\mathrm{T}} \left[\int_{\Omega} \left[B^{nl}\right]^{\mathrm{T}} [D] \left[B^{nl}\right] \mathrm{d}\Omega \right] \{\Delta U\} \\
& + \frac{1}{2} \{\Delta U\}^{\mathrm{T}} \left[\int_{\Omega} \nabla \left[B^{nl}\right]^{\mathrm{T}} l^2 [D] \nabla \left[B^{nl}\right] \mathrm{d}\Omega \right] \{\Delta U\} \\
& \{\Delta U\}^{\mathrm{T}} \int_{\Omega} \left[B^{nl}\right]^{\mathrm{T}} \{S_0\} \, \mathrm{d}\Omega + \{\Delta U\}^{\mathrm{T}} \int_{\Omega} [\varphi]^{\mathrm{T}} \rho [\varphi] \, \mathrm{d}\Omega \{\Delta \ddot{U}\} \\
& - \{\Delta U\}^{\mathrm{T}} \int_{\Gamma} [N]^{\mathrm{T}} \{\bar{t}\} \, \mathrm{d}\Gamma
\end{aligned} \tag{24}
$$

where '$\{\Delta U\}$' is the nodal displacement vector. The derivative of the total potential energy function with respect to the nodal displacement vector should be set to zero to minimize the potential energy function.

$$
\frac{\partial \Pi}{\partial \{\Delta U\}} = 0 \tag{25}
$$

Application of Eq. (25) to Eq. (24) yields to the mass matrix, tangent stiffness matrix and equivalent nodal load vector as follows.

$$
[M] = \int_{\Omega} [\varphi]^{\mathrm{T}} \rho [\varphi] \, \mathrm{d}\Omega \tag{26}
$$

$$
[K_{\mathrm{T}}] = \int_{\Omega} \left[B^{nl}\right]^{\mathrm{T}} [D] \left[B^{nl}\right] \mathrm{d}\Omega + \int_{\Omega} \nabla \left[B^{nl}\right]^{\mathrm{T}} l^2 [D] \nabla \left[B^{nl}\right] \mathrm{d}\Omega \tag{27}
$$

$$
\{\Delta P\} = \int_{\Gamma} [N]^{\mathrm{T}} \{\bar{t}\} \, \mathrm{d}\Gamma - \int_{\Omega} \left[B^{nl}\right]^{\mathrm{T}} \{S_0\} \, \mathrm{d}\Omega \tag{28}
$$

Thus, the nonlinear equation of motion which should be solved at the each time step is

$$
[M]\{\Delta \ddot{U}\} + [C]\{\Delta \dot{U}\} + [K_{\mathrm{T}}]\{\Delta U\} = \{\Delta P\} \tag{29}
$$

where '$[C]$' is the damping matrix which is constructed using Rayleigh method with respect to the mass and stiffness matrices (Rad *et al.* 2015). The Eq. (29) is nonlinear because the both side of this equation are function of nodal displacement. In the left side, the matrix $[K_T]$ is a function of nonlinear strain $[B^{nl}]$ matrix. According to the Eq. (18) the nonlinear strain matrix is defined with respect to deformation tensor which is a function of displacement. The right side of this equation is also a function of the initial second Piola–Kirchhoff stresses which is a function of nodal displacement. Thus, the nodal displacements must be computed using an incremental-iterative method. The solution procedure of Eq. (29) is presented in the next section.

6. Nonlinear Newmark-beta method

In the present paper, the combination of Newmark and Newton-Raphson methods is used for solving the time dependent nonlinear equations. The Newmark method involves solving the differential equations by a numerical time-stepping method. At each time step 'Δt', the following equations is used to approximate the acceleration and velocity vectors with respect to their values at the previous time step.

$$
\{\ddot{U}\}_{i+1} = \frac{1}{\beta(\Delta t)^2} \left(\{U\}_{i+1} - \{U\}_i \right) - \frac{1}{\beta(\Delta t)^2} \{\dot{U}\}_i - \left(\frac{1}{2\beta} - 1 \right) \{\ddot{U}\}_i \tag{30}
$$

$$
\{\dot{U}\}_{i+1} = \{\dot{U}\}_i + [(1-\gamma)\Delta t]\{\ddot{U}\}_i + \gamma \, \Delta t \, \{\ddot{U}\}_{i+1} \tag{31}
$$

where the parameters 'β' and 'γ' define the variation of acceleration over a time interval which are selected as 'β = 0.25' and 'γ = 0.5' corresponding to average acceleration at each time step. Substituting Eqs. (30) and (31) into equation of motion (Eq. (29)) one can obtains

$$
[\hat{K}_{\mathrm{T}}]\{\Delta U\}_i = \{\Delta \hat{P}\}_i \tag{32}
$$

where

$$\left[\hat{K}_{\mathrm{T}}\right]=\left[K_{\mathrm{T}}\right]+\frac{1}{\beta(\Delta t)^{2}}[M]+\frac{\gamma}{\beta(\Delta t)}[C] \tag{33}$$

and

$$\begin{aligned}\left\{\Delta\hat{P}\right\}_i &= \{\Delta P\}_i+\left(\frac{1}{\beta(\Delta t)^{2}}[M]+\frac{\gamma}{\beta(\Delta t)}[C]\right)\left\{\dot{U}\right\}_{i-1}\\ &+\left(\left(\frac{1}{2\beta}-1\right)[M]+\left(\frac{\gamma}{2\beta}-1\right)[C]\right)\left\{\ddot{U}\right\}_{i-1}\end{aligned} \tag{34}$$

In the solution of nonlinear quasi-static equation of motion at each time step (Eq. (32)), the well-known iterative Newton-Raphson technique is used. The Newmark/Newton-Raphson method can be implemented as a sequence of Fig. 2. This method is introduced in details in our previous published research (Rad *et al*. 2015).

7. Numerical results and discussions

In this section, the geometrically nonlinear analysis of a cantilever deep beam is carried out by proposed method. The schematic of the problem is shown in Fig. 3.

The initial Lame constants of the material are considered as ‘μ_0 = 0.5×10^4 Pa’ and ‘λ_0 = 3.3×10^3 Pa’ and the mass density is ‘ρ = 2.2 gr/cm^3’.

7.1 Static analysis

To verify the accuracy of proposed model, the pre-mentioned beam is analyzed at a large scale (‘L = 10 m’ and ‘H = 2 m’) without considering small scale effect (l = 0). The beam is considered under uniform distributed incremental shear stress at the free end. The applied stress tension at the nth loading step is defined as (Gu *et al*. 2007).

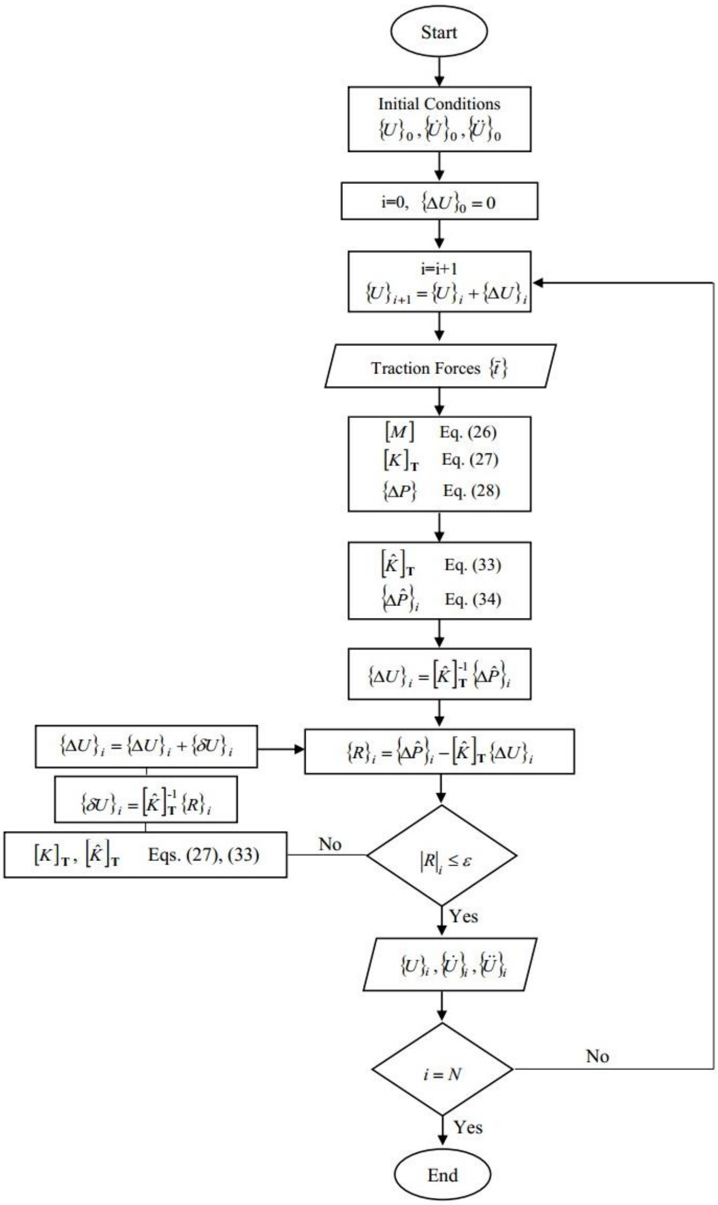

Fig. 2 Flow chart for large deformation analysis of nanostructures using EFG method

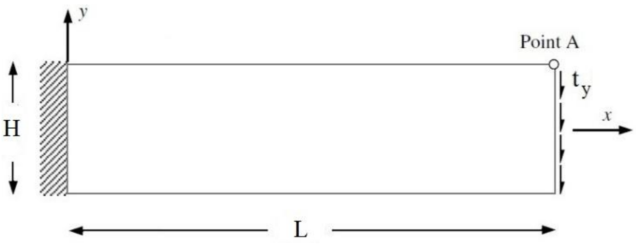

Fig. 3 The geometry and boundary conditions of the cantilever beam

$$T_y(n) = \beta \times n \left(\frac{\mathrm{N}}{\mathrm{m}^2}\right) \tag{35}$$

where 'β' is the load scale factor which is considered to be 'β = 10' and loading is applied in eight steps. The vertical displacement of point 'A' at the all load steps are listed in Table 1, for various nodal distributions. The results obtained using finite element method by Gu *et al*. (2007) are also reported in this table. It is observed that the results of presented EFG method with '16×8' nodal distribution are in good agreement with those obtained using finite element method with the very fine mesh (738 nodes).

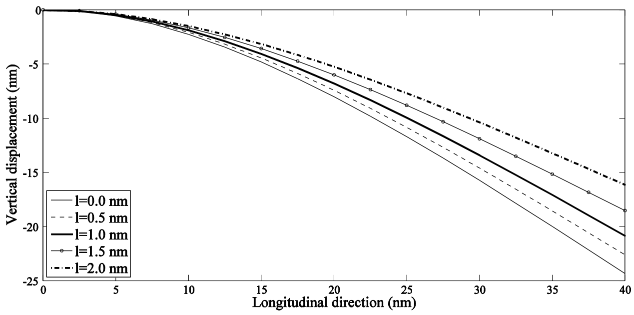

Fig. 4 Midline vertical displacement at the end of load steps

In Table 1, the percentage difference of the EFG method with the FEM is obtained from the following equation.

$$\text{dif } (\%) = \left|\frac{v^{FEM} - v^{EFG}}{v^{FEM}}\right| \times 100 \tag{36}$$

In the next example, the dimensions of the beam are considered as 'L = 40 nm' and 'H = 8 nm' to investigate the small scale effect. The load is increased by 10 load steps. The midline vertical displacement of the cantilever beam for various values of the nonlocal parameter at the end load

Table 1 Vertical displacement of point 'A' without nonlocality effect obtained from EFG with various nodal distribution comparing with the FEM (Gu *et al*. 2007)

Load step (n)		1	2	3	4	5	6	7	8
FEM (Gu *et al*. 2007)	$-v_A$ (m)	0.816	1.617	2.376	3.078	3.714	4.283	4.768	5.235
Present (8×4)	$-v_A$ (m)	0.816	1.617	2.376	3.078	3.714	4.283	4.768	5.235
	$-v_A$ (m)	0.707	1.416	2.106	2.760	3.368	3.929	4.435	4.901
Present (12×4)	dif (%)	13.36	12.43	11.36	10.33	9.32	8.27	6.98	6.38
	$-v_A$ (m)	0.747	1.494	2.219	2.903	3.539	4.119	4.641	5.122
Present (12×6)	dif (%)	8.46	7.61	6.61	5.69	4.71	3.83	2.66	2.16
	$-v_A$ (m)	0.742	1.484	2.204	2.885	3.516	4.094	4.614	5.088
Present (16×6)	dif (%)	9.07	8.23	7.24	6.27	5.33	4.41	3.23	2.81
	$-v_A$ (m)	0.799	1.596	2.366	3.089	3.756	4.359	4.907	5.393
Present (16×8)	dif (%)	2.08	1.30	0.42	0.36	1.13	1.77	2.92	3.02
	$-v_A$ (m)	0.776	1.552	2.302	3.008	3.660	4.252	4.790	5.271

Table 2 The effect of nonlocal parameter on maximum vertical displacement at the all load steps

Load step (n)		1	2	3	4	5	6	7	8
l = 0.0	$-v_A$ (m)	3.194	6.384	9.465	12.358	15.014	17.414	19.554	21.445
l = 0.5 (nm)	$-v_A$ (m)	3.030	6.059	8.997	11.770	14.336	16.671	18.772	20.645
	$-v_A$ (m)	5.13	5.09	4.94	4.76	4.52	4.27	4.00	3.73
l = 1.0 (nm)	dif (%)	2.659	5.323	7.927	10.419	12.761	14.932	16.922	18.733
	$-v_A$ (m)	16.75	16.62	16.25	15.69	15.01	14.25	13.46	12.64
l = 1.5 (nm)	dif (%)	2.238	4.482	6.694	8.840	10.893	12.835	14.654	16.345
	$-v_A$ (m)	29.93	29.79	29.28	28.47	27.45	26.29	25.06	23.78
l = 2.0 (nm)	dif (%)	1.855	3.717	5.563	7.373	9.129	10.818	12.430	13.959
	$-v_A$ (m)	41.92	41.78	41.23	40.34	39.20	37.88	36.43	34.91

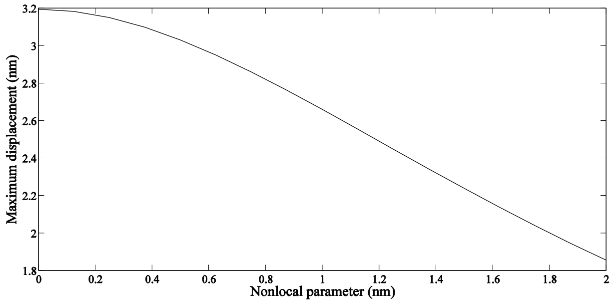

Fig. 5 Effect of nonlocal parameter on maximum vertical displacement

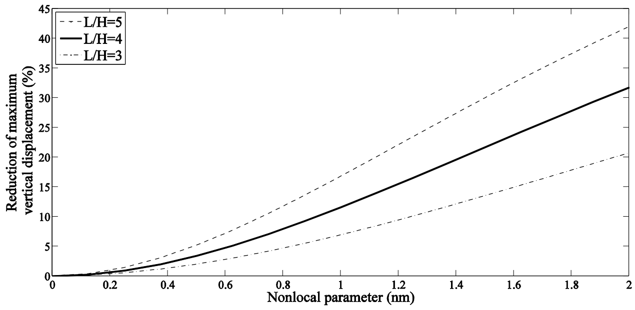

Fig. 6 Effect of aspect ratio on small scale effect

step is compared with the local ones in Fig. 4. According to this figure, it can be seen that for this problem the displacement decreases with increase nonlocal parameter.

The variation of the maximum displacement of the beam with respect to the nonlocal parameter for all load steps is shown in Table 2.

Based on this table, it can be concluded that at the higher load steps the effect of nonlocality is decreased. For example, by increasing the nonlocal parameter from 'l = 0' to 'l = 2 nm', the maximum displacement approximately decreases by 42% and 32% at the first and end load steps, respectively.

In Fig. 5, the maximum vertical displacement of the beam is plotted as a function of the nonlocal parameter at the first load step. It should be mentioned that the nonlocal parameters is defined as '$l = e_0 a$' where 'e_0' is a constant which varies accordance with each material and the parameter 'a' is the internal characteristic length (e.g., the length of C-C bounds) obtained by experience or matching dispersion curves of plane waves with those of atomic lattice dynamics (Arash and Ansari 2010). It is obvious that the local elasticity is retrieved when the nonlocal parameter becomes zero. According to Fig. 4, it can be observed that by increasing the nonlocal parameter, the maximum vertical displacement is decreased. In other words, the nonlocal parameter directly effects on stiffness of nanostructures (See Eq. (27)). The maximum rate of decrease in vertical displacement with increase the nonlocal parameter (maximum slope of the diagram) is related to 'l = 1.2 nm'.

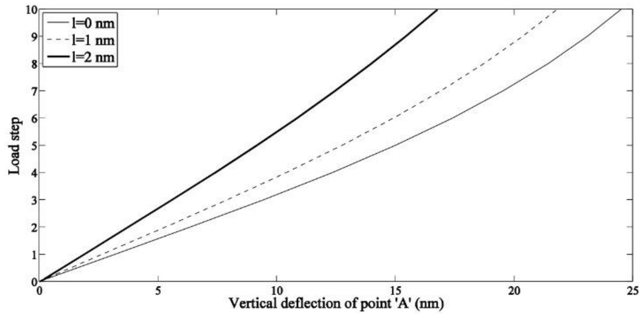

Fig. 7 Load versus vertical deflection of point 'A' for various nonlocal parameters

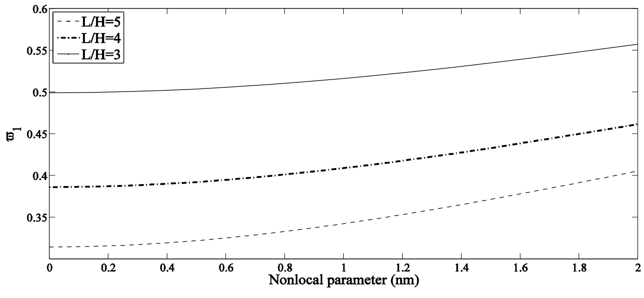

(a) 1st mode

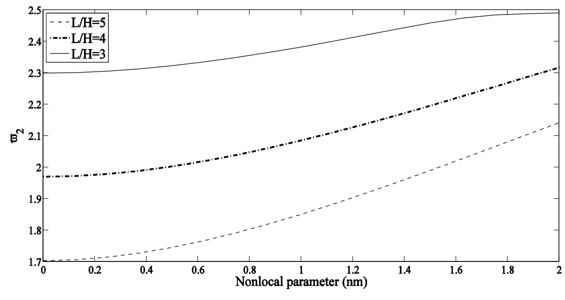

(b) 2nd mode

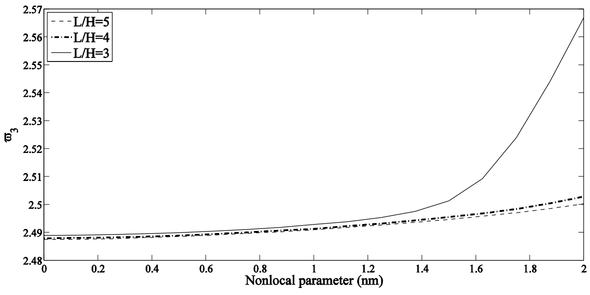

(c) 3rd mode

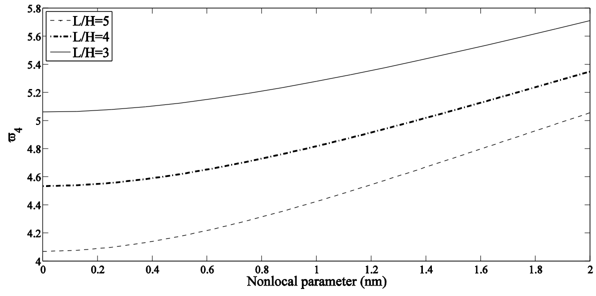

(d) 4th mode

Fig. 8 Effect of nonlocal parameter on natural frequencies

The same results are achieved at the other load steps.

In Fig. 6, the diagram of percentage reduction of maximum vertical displacement due to nonlocality versus the nonlocal parameter is presented. It is assumed that the length of the cylinder is constant 'L = 40 nm' and this diagram is plotted for various length to height 'L/H' ratios. As can be seen in this figure, by increasing the value of 'L/H', the small scale effect is increased.

The vertical displacement of point 'A' versus the load steps for various nonlocal parameter is shown in Fig. 7. According to this figure, it is clear that the beam has been entered the geometry's nonlinear region.

7.2 Dynamic analysis

In what follows, the introduced beam in previous subsection, is analyzed under impact loading. The effects of structural parameters such as nonlocal parameter and aspect ratio on dynamic behavior of the beam are studied. The beam is subjected to the following ramp stress at the free end.

$$T_y(t) = \begin{cases} 2\times10^6\, t & t \le 2\times10^{-6}\ s \\ 0 & t > 2\times10^{-6}\ s \end{cases} \tag{37}$$

The effect of nonlocal parameter on natural frequencies of the beam at the initial state for various length to height ratios are shown in Fig. 8. In this figure dimensionless natural frequencies are defined as

$$\varpi_i = \left(L\sqrt{\frac{\rho}{\mu_0}} \right)\omega_i \tag{38}$$

According to Fig. 8, it can be seen that for all vibration modes and aspect ratios, the natural frequencies are increased by increasing in nonlocal parameter. The values of dimensionless natural frequencies for various length to height ratios and nonlocal parameters are listed in Table 3.

Table 3 Dimensionless natural frequencies for different values of aspect ratio and nonlocal parameter

Nonlocal parameter (nm)		l = 0.0	l = 0.5	l = 1.0	l = 1.5	l = 2.0
L/H = 3	ϖ_1	0.4989	0.5035	0.5161	0.5346	0.5572
	ϖ_2	2.2983	2.3218	2.3813	2.4578	2.4901
	ϖ_3	2.4889	2.4899	2.4928	2.5013	2.5668
	ϖ_4	5.0608	5.1237	5.2785	5.4822	5.7107
L/H = 4	ϖ_1	0.3863	0.3924	0.4091	0.4332	0.4619
	ϖ_2	1.9704	2.0031	2.0855	2.1958	2.3174
	ϖ_3	2.4880	2.489	2.4914	2.4956	2.5029
	ϖ_4	4.5362	4.6201	4.8203	5.0753	5.3509
L/H = 5	ϖ_1	0.3141	0.3217	0.3420	0.3712	0.4052
	ϖ_2	1.7025	1.7445	1.8496	1.9888	2.1409
	ϖ_3	2.4875	2.4885	2.4909	2.4946	2.5002
	ϖ_4	4.0689	4.1754	4.4238	4.7325	5.0556

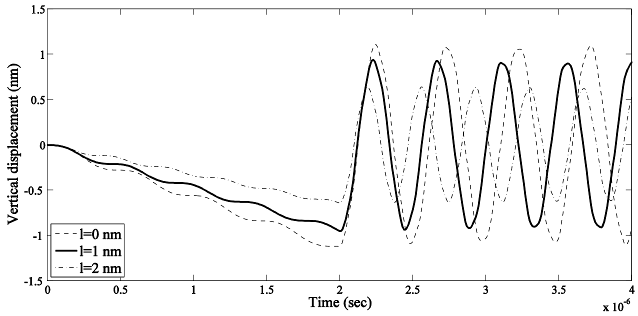

Fig. 9 Vertical displacement time history of point 'A' for various nonlocal parameter

In Fig. 9, the time histories of point 'A' for various nonlocal parameter are plotted. According to this figure, it can be seen that as the nonlocal parameter increases the maximum vertical displacement and the period of vibration is decreased.

Figs. 10 and 11 represent the effect of damping ratio on time history of point 'A' for 'l = 0' and 'l = 2 nm', respectively. By comparing these figures one can conclude that considering small scale effect yields to increasing the rate of vibration decays due to damping. In addition, according to Figs. 10 and 11 it is obvious that the damping ratio has no significant effect on period of vibration in free vibration section.

In the next example, the beam is subjected to the following sinusoidal loading.

$$T_y(t) = F_0 \sin\left(\frac{\pi}{T} t\right) \tag{39}$$

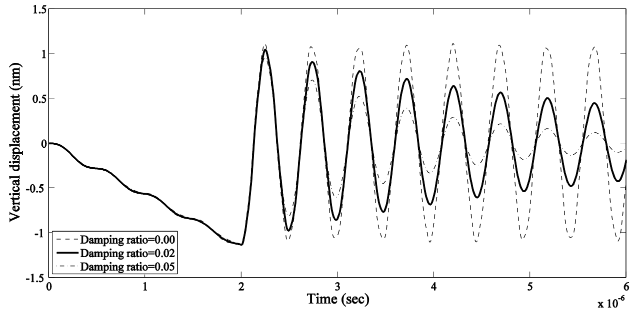

Fig. 10 Vertical displacement time history of point 'A' for 'l = 0' and various damping ratio

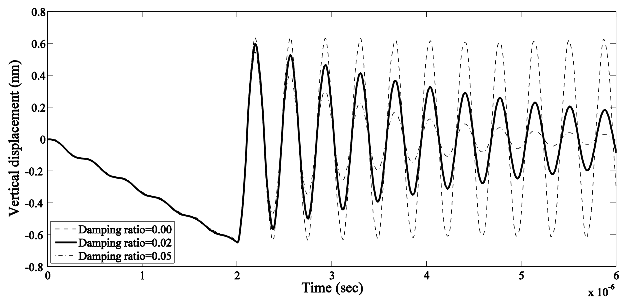

Fig. 11 Vertical displacement time history of point 'A' for 'l = 2 m' and various damping ratio

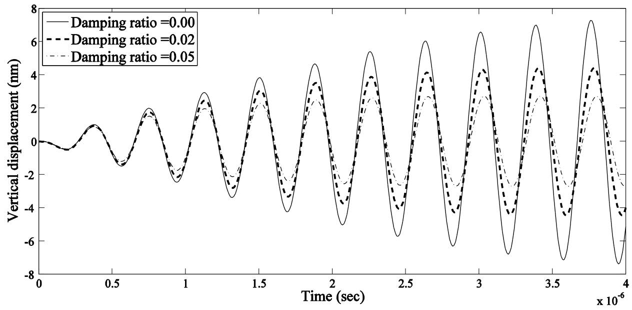

Fig. 12 Vertical displacement time history of point ‘A’ under sinusoidal loading

where ‘$F_0 = 2$ N/m^2’ and ‘$T = 1.9e - 7$s’. Fig. 12 shows the time histories of point ‘A’ for ‘ $l = 2$ nm’ and various damping ratios. As can be observed in this figure, since the forcing frequency is near the natural frequency of the beam, the amplitude of vibration becomes higher and higher with each vibration (resonance). However, damping reduces the effect of resonance by decreasing the increment of vibration amplitude. In addition according to this figure, it can be concluded that in forced vibration, the damping ratio slightly affect the vibration frequency.

8. Conclusions

This paper has presented a geometrically nonlinear dynamic analysis of the neo-Hookean micro/nano deep beams using the EFG method. The gradient nonlocal continuum theory is used to derive the nonlocal differential equations. The nonlinear dynamic equation of motion is obtained by minimization of total potential energy at the initial configuration (total Lagrangian approach). To develop the discretized system of equations, the EFG method is employed. The multi-quadric radial basis function is used for construction the shape functions. The governing equations is solved by incremental- iterative Newmark-Newton method with the small load steps. Several numerical simulations are performed and the important results are outlined as follows.

- The geometrically nonlinear results of EFG method with ‘16×8’ nodal distribution are in good agreement with those obtained using finite element method with the very fine mesh.
- Increasing the length to height ratio causes to increase the small scale effect.
- The natural frequencies of the cantilever beam are increased by increasing in nonlocal parameter at the all vibration modes.
- The deflections of the cantilever deep beam and the period of vibration decreases with increase the nonlocal parameter. In the other words, the stiffness of the cantilever beam is increased due to the small scale effects.
- The vibration decays due to damping effect is increased by increasing the nonlocal parameter.
- When the forcing frequency is near the natural frequency of the beam, the amplitude of vibration become higher and higher with each vibration (resonance). The resonance effect is decreased by increasing the damping ratio.
- In forced vibration problems, the damping ratio slightly affects the frequency of vibration.

References

Aifantis, E.C. (1999), “Strain gradient interpretation of size effects”, In: *Fracture Scaling*, Springer, Dordrecht, pp. 299-314.

Akgöz, B. and Civalek, Ö. (2011), “Strain gradient elasticity and modified couple stress models for buckling analysis of axially loaded micro-scaled beams”, *Int. J. Eng. Sci.*, **49**(11), 1268-1280. https://doi.org/10.1016/j.ijengsci.2010.12.009

Altan, B.S. and Aifantis, E.C. (1997), “On some aspects in the special theory of gradient elasticity”, *J. Mech. Behavior Mater.*, **8**(3), 231-282. https://doi.org/10.1515/JMBM.1997.8.3.231

Amanatidou, E. and Aravas, N. (2002), “Mixed finite element formulations of strain-gradient elasticity problems”, *Comput. Methods Appl. Mech. Eng.*, **191**(15-16), 1723-1751. https://doi.org/10.1016/S0045-7825(01)00353-X

Arash, B. and Ansari, R. (2010), “Evaluation of nonlocal parameter in the vibrations of single-walled carbon nanotubes with initial strain”, *Physica E: Low-dimens. Syst. Nanostruct.*, **42**(8), 2058-2064. https://doi.org/10.1016/j.physe.2010.03.028

Arefi, M. (2018), “Nonlocal free vibration analysis of a doubly curved piezoelectric nano shell”, *Steel Compos. Struct., Int. J.*, **27**(4), 479-493. https://doi.org/10.12989/scs.2018.27.4.479

Askes, H. and Aifantis, E.C. (2002), “Numerical modeling of size effects with gradient elasticity-formulation, meshless discretization and examples”, *Int. J. Fract.*, **117**(4), 347-358. https://doi.org/10.1023/A:1022225526483

Belytschko, T., Gracie, R. and Ventura, G. (2009), “A review of extended/generalized finite element methods for material modeling”, *Model. Simul. Mater. Sci. Eng.*, **17**(4), 043001. https://doi.org/10.1088/0965-0393/17/4/043001

Cadek, M., Coleman, J.N., Ryan, K.P., Nicolosi, V., Bister, G., Fonseca, A. and Blau, W.J. (2004), “Reinforcement of polymers with carbon nanotubes: the role of nanotube surface area”, *Nano Letters*, **4**(2), 353-356. https://doi.org/10.1021/nl035009o

Chakraverty, S. and Behera, L. (2015), “Small scale effect on the vibration of non-uniform nanoplates”, *Struct. Eng. Mech., Int. J.*, **55**(3), 495-510. https://doi.org/10.12989/sem.2015.55.3.495

Chen, W.X., Tu, J.P., Wang, L.Y., Gan, H.Y., Xu, Z.D. and Zhang, X.B. (2003), “Tribological application of carbon nanotubes in a metal-based composite coating and composites”, *Carbon*, **41**(2), 215-222. https://doi.org/10.1016/S0008-6223(02)00265-8

Chong, A.C.M., Yang, F., Lam, D.C. and Tong, P. (2001), “Torsion and bending of micron-scaled structures”, *J. Mater. Res.*, **16**(4), 1052-1058. https://doi.org/10.1557/JMR.2001.0146

Darabi, A. and Vosoughi, A.R. (2016), “A hybrid inverse method for small scale parameter estimation of FG nanobeams”, *Steel Compos. Struct., Int. J.*, **20**(5), 1119-1131. https://doi.org/10.12989/scs.2016.20.5.1119

Despotovic, N. (2018), “Stability and vibration of a nanoplate under body force using nonlocal elasticity theory”, *Acta Mechanica*, **229**(1), 273-284. https://doi.org/10.1007/s00707-017-1962-9

Eringen, A.C. (1972a), “Linear theory of nonlocal elasticity and dispersion of plane waves”, *Int. J. Eng. Sci.*, **10**(5), 425-435. https://doi.org/10.1016/0020-7225(72)90050-X

Eringen, A.C. (1972b), “Nonlocal polar elastic continua”, *Int. J. Eng. Sci.*, **10**(1), 1-16.

https://doi.org/10.1016/0020-7225(72)90070-5

Eltaher, M.A., Khater, M.E. and Emam, S.A. (2016), "A review on nonlocal elastic models for bending, buckling, vibrations, and wave propagation of nanoscale beams", *Appl. Math. Model.*, **40**(5-6), 4109-4128. https://doi.org/10.1016/j.apm.2015.11.026

Ghavanloo, E. and Fazelzadeh, S.A. (2016), "Evaluation of nonlocal parameter for single-walled carbon nanotubes with arbitrary chirality", *Meccanica*, **51**(1), 41-54. https://doi.org/10.1007/s11012-015-0195-z

Gholami, R. and Ansari, R. (2016), "A most general strain gradient plate formulation for size-dependent geometrically nonlinear free vibration analysis of functionally graded shear deformable rectangular microplates", *Nonlinear Dyn.*, **84**(4), 2403-2422. https://doi.org/10.1007/s11071-016-2653-0

Gu, Y., Wang, Q.X. and Lam, K.Y. (2007), "A meshless local Kriging method for large deformation analyses", *Comput. Methods Appl. Mech. Eng.*, **196**(9-12), 1673-1684. https://doi.org/10.1016/j.cma.2006.09.017

Hosseini, S.M. (2018), "Analytical solution for nonlocal coupled thermoelasticity analysis in a heat-affected MEMS/NEMS beam resonator based on Green–Naghdi theory", *Appl. Math. Model.*, **57**, 21-36. https://doi.org/10.1016/j.apm.2017.12.034

Hosseini, S.M. and Zhang, C. (2018a), "Coupled thermoelastic analysis of an FG multilayer graphene platelets-reinforced nanocomposite cylinder using meshless GFD method: A modified micromechanical model", *Eng. Anal. Boundary Elem.*, **88**, 80-92. https://doi.org/10.1016/j.enganabound.2017.12.010

Hosseini, S.M. and Zhang, C. (2018b), "Elastodynamic and wave propagation analysis in a FG graphene platelets-reinforced nanocomposite cylinder using a modified nonlinear micromechanical model", *Steel Compos. Struct., Int. J.,* **27**(3), 255-271. https://doi.org/10.12989/scs.2018.27.3.255

Kiani, K. (2014), "A nonlocal meshless solution for flexural vibrations of double-walled carbon nanotubes", *Appl. Math. Computat.*, **234**, 557-578. https://doi.org/10.1016/j.amc.2014.01.015

Lam, D.C., Yang, F., Chong, A.C.M., Wang, J. and Tong, P. (2003), "Experiments and theory in strain gradient elasticity", *J. Mech. Phys. Solids*, **51**(8), 1477-1508. https://doi.org/10.1016/S0022-5096(03)00053-X

Lei, Z.X., Zhang, L.W., Liew, K.M. and Yu, J.L. (2014), "Dynamic stability analysis of carbon nanotube-reinforced functionally graded cylindrical panels using the element-free kp-Ritz method", *Compos. Struct.*, **113**, 328-338. https://doi.org/10.1016/j.compstruct.2014.03.035

Lei, Z.X., Zhang, L.W. and Liew, K.M. (2015), "Free vibration analysis of laminated FG-CNT reinforced composite rectangular plates using the kp-Ritz method", *Compos. Struct.*, **127**, 245-259. https://doi.org/10.1016/j.compstruct.2015.03.019

Liu, G.R. and Gu, Y.T. (2005), *An introduction to meshfree methods and their programming*, Springer Science & Business Media.

Ma, Q. and Clarke, D.R. (1995), "Size dependent hardness of silver single crystals", *J. Mater. Res.*, **10**(4), 853-863. DOI: https://doi.org/10.1557/JMR.1995.0853

Malekzadeh, P. and Shojaee, M. (2013), "Surface and nonlocal effects on the nonlinear free vibration of non-uniform nanobeams", *Compos. Part B: Eng.*, **52**, 84-92. https://doi.org/10.1016/j.compositesb.2013.03.046

Mindlin, R.D. (1964), "Micro-structure in linear elasticity", *Archive Rational Mech. Anal.*, **16**(1), 51-78. https://doi.org/10.1007/BF00248490

Mirjavadi, S.S., Afshari, B.M., Shafiei, N., Hamouda, A.M.S. and Kazemi, M. (2017), "Thermal vibration of two-dimensional functionally graded (2D-FG) porous Timoshenko nanobeams", *Steel Compos. Struct., Int. J.*, **25**(4), 415-426. https://doi.org/10.12989/scs.2017.25.4.415

Nguyen, T.N., Kim, N.I. and Lee, J. (2017), "Static behavior of nonlocal Euler-Bernoulli beam model embedded in an elastic medium using mixed finite element formulation", *Struct. Eng. Mech., Int. J.*, **63**(2), 137-146. https://doi.org/10.12989/sem.2017.63.2.137

Nikkar, A., Rouhi, S. and Ansari, R. (2017), "Finite element modeling of the vibrational behavior of multi-walled nested silicon-carbide and carbon nanotubes", *Struct. Eng. Mech., Int. J.*, **64**(3), 329-337. https://doi.org/10.12989/sem.2017.64.3.329

Panyatong, M., Chinnaboon, B. and Chucheepsakul, S. (2018), "Nonlinear bending analysis of nonlocal nanoplates with general shapes and boundary conditions by the boundary-only method", *Eng. Anal. Boundary Elem.*, **87**, 90-110. https://doi.org/10.1016/j.enganabound.2017.12.003

Phadikar, J.K. and Pradhan, S.C. (2010), "Variational formulation and finite element analysis for nonlocal elastic nanobeams and nanoplates", *Computat. Mater. Sci.*, **49**(3), 492-499. https://doi.org/10.1016/j.commatsci.2010.05.040

Polizzotto, C. (2001), "Nonlocal elasticity and related variational principles", *Int. J. Solids Struct.*, **38**(42-43), 7359-7380. https://doi.org/10.1016/S0020-7683(01)00039-7

Poole, W.J., Ashby, M.F. and Fleck, N.A. (1996), "Micro-hardness of annealed and work-hardened copper polycrystal", *Scripta Materialia*, **34**(4), 559-564.

Rad, M.H.G., Shahabian, F. and Hosseini, S.M. (2015), "A meshless local Petrov–Galerkin method for nonlinear dynamic analyses of hyper-elastic FG thick hollow cylinder with Rayleigh damping", *Acta Mechanica*, **226**(5), 1497-1513. https://doi.org/10.1007/s00707-014-1266-2

Rahmani, O., Refaeinejad, V. and Hosseini, S.A.H. (2017), "Assessment of various nonlocal higher order theories for the bending and buckling behavior of functionally graded nanobeams", *Steel Compos. Struct., Int. J.*, **23**(3), 339-350. https://doi.org/10.12989/scs.2017.23.3.339

Reddy, J.N. (2010), "Nonlocal nonlinear formulations for bending of classical and shear deformation theories of beams and plates", *Int. J. Eng. Sci.*, **48**(11), 1507-1518. https://doi.org/10.1016/j.ijengsci.2010.09.020

Schwartz, M., Niane, N.T. and Njiwa, R.K. (2012), "A simple solution method to 3D integral nonlocal elasticity: Isotropic-BEM coupled with strong form local radial point interpolation", *Eng. Anal. Boundary Elem.*, **36**(4), 606-612. https://doi.org/10.1016/j.enganabound.2011.10.004

Sladek, J., Sladek, V., Hrcek, S. and Pan, E. (2017), "The nonlocal and gradient theories for a large deformation of piezoelectric nanoplates", *Compos. Struct.*, **172**, 119-129. https://doi.org/10.1016/j.compstruct.2017.03.080

Taghizadeh, M., Ovesy, H.R. and Ghannadpour, S.A.M. (2015), "Nonlocal integral elasticity analysis of beam bending by using finite element method", *Struct. Eng. Mech., Int. J.*, **54**(4), 755-769. https://doi.org/10.12989/sem.2015.54.4.755

Toupin, R.A. (1964), "Theories of elasticity with couple-stress", *Archive Rational Mech. Anal.*, **17**(2), 85-112. https://doi.org/10.1007/BF00253050

Wang, K.F., Wang, B.L. and Kitamura, T. (2016), "A review on the application of modified continuum models in modeling and simulation of nanostructures", *Acta Mechanica Sinica*, **32**(1), 83-100. https://doi.org/10.1007/s10409-015-0508-4

Wang, L., He, X., Sun, Y. and Liew, K.M. (2017a), "A mesh-free vibration analysis of strain gradient nano-beams", *Eng. Anal. Bound. Elem.*, **84**, 231-236. https://doi.org/10.1016/j.enganabound.2017.09.001

Wang, Y., Li, F., Wang, Y. and Jing, X. (2017b), "Nonlinear responses and stability analysis of viscoelastic nanoplate resting on elastic matrix under 3: 1 internal resonances", *Int. J. Mech. Sci.*, **128**, 94-104. https://doi.org/10.1016/j.ijmecsci.2017.04.010

Wang, Y., Li, F.M. and Wang, Y.Z. (2015a), "Homoclinic behaviors and chaotic motions of double layered viscoelastic nanoplates based on nonlocal theory and extended Melnikov method", *Chaos*: *An Interdiscipl*. *J*. *Nonlinear Sci*., **25(**6), 063108. https://doi.org/10.1063/1.4922299

Wang, Y., Li, F.M. and Wang, Y.Z. (2015b), "Nonlinear vibration of double layered viscoelastic nanoplates based on nonlocal theory", *Physica E*: *Low-dimens*. *Syst*. *Nanostruct*., **67**, 65-76. https://doi.org/10.1016/j.physe.2014.11.007

Wang, Y.Z., Li, F.M. and Kishimoto, K. (2010), "Scale effects on the longitudinal wave propagation in nanoplates", *Physica E*: *Low-dimens*. *Syst*. *Nanostruct*., **42**(5), 1356-1360. https://doi.org/10.1016/j.physe.2009.11.036

Wang, Y., Li, F. and Shu, H. (2019), "Nonlocal nonlinear chaotic and homoclinic analysis of double layered forced viscoelastic nanoplates", *Mech*. *Syst*. *Signal Process*., **122**, 537-554. https://doi.org/10.1016/j.ymssp.2018.12.041

Yang, F.A.C.M., Chong, A.C.M., Lam, D.C.C. and Tong, P. (2002), "Couple stress based strain gradient theory for elasticity", *Int*. *J*. *Solids Struct*., **39**(10), 2731-2743. https://doi.org/10.1016/S0020-7683(02)00152-X

Yu, Y.J., Xue, Z.N., Li, C.L. and Tian, X.G. (2016), "Buckling of nanobeams under nonuniform temperature based on nonlocal thermoelasticity", *Compos*. *Struct*., **146**, 108-113. https://doi.org/10.1016/j.compstruct.2016.03.014

Yu, Y.J., Tian, X.G. and Liu, J. (2017), "Size-dependent damping of a nanobeam using nonlocal thermoelasticity: extension of Zener, Lifshitz, and Roukes' damping model", *Acta Mechanica*, **228**(4), 1287-1302. https://doi.org/10.1007/s00707-016-1769-0

Zhang, L.W. (2017), "An element-free based IMLS-Ritz method for buckling analysis of nanocomposite plates of polygonal planform", *Eng*. *Anal*. *Boundary Elem*., **77**, 10-25. https://doi.org/10.1016/j.enganabound.2015.01.007

Zhang, L.W. and Liew, K.M. (2015), "Large deflection analysis of FG-CNT reinforced composite skew plates resting on Pasternak foundations using an element-free approach", *Compos*. *Struct*., **132**, 974-983. https://doi.org/10.1016/j.compstruct.2015.07.017

Zhang, L.W. and Liew, K.M. (2016), "Postbuckling analysis of axially compressed CNT reinforced functionally graded composite plates resting on Pasternak foundations using an element-free approach", *Compos. Struct*., **138**, 40-51. https://doi.org/10.1016/j.compstruct.2015.11.031

Zhang, L.W. and Selim, B.A. (2017), "Vibration analysis of CNT-reinforced thick laminated composite plates based on Reddy's higher-order shear deformation theory", *Compos*. *Struct*., **160**, 689-705. https://doi.org/10.1016/j.compstruct.2016.10.102

Zhang, L.W. and Xiao, L.N. (2017), "Mechanical behavior of laminated CNT-reinforced composite skew plates subjected to dynamic loading", *Compos*. *Part B*: *Eng*., **122**, 219-230. https://doi.org/10.1016/j.compositesb.2017.03.041

Zhang, L.W., Zhu, P. and Liew, K.M. (2014), "Thermal buckling of functionally graded plates using a local Kriging meshless method", *Compos*. *Struct*., **108**, 472-492. https://doi.org/10.1016/j.compstruct.2013.09.043

Zhang, L.W., Song, Z.G. and Liew, K.M. (2015a), "State-space Levy method for vibration analysis of FG-CNT composite plates subjected to in-plane loads based on higher-order shear deformation theory", *Compos*. *Struct*., **134**, 989-1003. https://doi.org/10.1016/j.compstruct.2015.08.138

Zhang, L.W., Li, D.M. and Liew, K.M. (2015b), "An element-free computational framework for elastodynamic problems based on the IMLS-Ritz method", *Eng*. *Anal*. *Boundary Elem*., **54,** 39-46. https://doi.org/10.1016/j.compstruct.2015.11.031

Zhang, L.W., Liu, W.H. and Liew, K.M. (2016a), "Geometrically nonlinear large deformation analysis of triangular CNT-reinforced composite plates", *Int*. *J*. *Non-Linear Mech*., **86**, 122-132. https://doi.org/10.1016/j.ijnonlinmec.2016.08.004

Zhang, L.W., Song, Z.G. and Liew, K.M. (2016b), "Computation of aerothermoelastic properties and active flutter control of CNT reinforced functionally graded composite panels in supersonic airflow", *Comput*. *Methods Appl*. *Mech*. *Eng*., **300**, 427-441. https://doi.org/10.1016/j.cma.2015.11.029

Zhang, Y., Zhang, L.W., Liew, K.M. and Yu, J.L. (2016c), "Buckling analysis of graphene sheets embedded in an elastic medium based on the kp-Ritz method and non-local elasticity theory", *Eng*. *Anal*. *Boundary Elem*., **70**, 31-39. https://doi.org/10.1016/j.enganabound.2016.05.009

Zhang, L.W., Liew, K.M. and Reddy, J.N. (2016d), "Postbuckling of carbon nanotube reinforced functionally graded plates with edges elastically restrained against translation and rotation under axial compression", *Comput*. *Methods Appl*. *Mech*. *Eng*., **298**, 1-28. https://doi.org/10.1016/j.cma.2015.09.016

Zhang, L.W., Song, Z.G. and Liew, K.M. (2016e), "Optimal shape control of CNT reinforced functionally graded composite plates using piezoelectric patches", *Compos*. *Part B*: *Eng*., **85**, 140-149. https://doi.org/10.1016/j.compositesb.2015.09.044

Zhang, L.W., Song, Z.G., Qiao, P. and Liew, K.M. (2017), "Modeling of dynamic responses of CNT-reinforced composite cylindrical shells under impact loads", *Comput*. *Methods Appl*. *Mech*. *Eng*., **313**, 889-903. https://doi.org/10.1016/j.cma.2016.10.020

Zhu, P., Zhang, L.W. and Liew, K.M. (2014), "Geometrically nonlinear thermomechanical analysis of moderately thick functionally graded plates using a local Petrov–Galerkin approach with moving Kriging interpolation", *Compos*. *Struct*., **107**, 298-314. https://doi.org/10.1016/j.compstruct.2013.08.001

CC